CAV2021
11th International Symposium on Cavitation
May 10-13, 2021, Daejon, Korea

A Comparative Study on the Static Pressure Limit for Acoustically-Driven Bubble and Laser-Induced Bubble

Kewen Peng [1, 2]*, Frank G. F. Qin[2], Shouceng Tian[1] and Yiqun Zhang [1]

[1] State Key Laboratory of Petroleum Resources and Prospecting, China University of Petroleum-Beijing, China
[2] Guangdong Provincial Key Laboratory of Distributed Energy Systems, School of Chemical Engineering and Energy Technology, Dongguan University of Technology, China

Abstract: Two pioneering experiments have demonstrated opposite effects of ambient pressure on single bubble sonoluminescence (SBSL): for acoustically-driven bubbles (ADB) a certain degree of vacuum promotes SBSL [Dan *et al*., Phys. Rev. Lett. 83(9), 1870, (1999)], while for laser-induced bubbles (LIB) imposing elevated static pressure achieves similar performance (Baghdassarian *et al*., Phys. Rev. Lett. 83(12), 2437, (1999)]. Both methods, however, share the same constraint: bubble spherical shape instability limits the extent of vacuuming or pressurization. In this paper, we theoretically predict those limits according to the calculation of surface instabilities for these two kinds of bubbles. The calculation is based on the phase diagrams for sonoluminescing bubbles under different ambient pressures. We showed the characteristics of the parametric and Rayleigh-Taylor instability developed on ADB and LIB, respectively. The narrow range of stable region for ADB indicates its sensitivity to the variation of the ambient condition. In contrast, the large-sized LIB is rather stable and its luminescence intensity can be significantly enhanced by imposing high static pressure up to several bars

Keywords: bubble stability; static pressure; acoustically-driven bubbles; laser-induced bubbles

1. Introduction

The phenomenon of light emission from an acoustically levitated bubble has intrigued scientists for a long time, reinforced notably by the classic experiment of Gaitan [1]. Apart from theoretically modeling the involved hydrodynamic, chemical, and atomic processes directly, an alternative approach to probe this phenomenon is to vary external conditions surrounding the bubble and then observe the change in the luminescence. The most studied parameter is liquid temperature, as summarized in Ref.[2]. Previous investigators also examined the influence of static pressure. Their results show an interesting and diverging pattern for two kinds of bubbles: for the acoustically-driven bubbles (ADB), the decrease of static pressure below the atmosphere leads to the enhanced sonoluminescence[3], while for laser-induced bubbles (LIB), this trend is reversed, i.e., the augmentation of light emission can be caused by imposing higher pressure than atmospheric value[4, 5]. In the experiments, both methods shared a constraint in pursuing stronger luminescence: bubble instability. In this paper, we leave out the mechanism analysis of the pressure effect, and, instead, focus on the latter. We study the characteristics of instability for the two categories of bubbles and predict the boundaries of the allowable vacuuming or pressurization. We aim to contribute more insights to the broad subject of sonoluminescence.

2. The numerical model

* Corresponding Author: Kewen Peng, pengkw@dgut.edu.cn

We followed the classic approach proposed by Hilgenfeldt et al[6] and Hao and Prosperetti[7] to investigate the bubble instability developed on the bubble surface. The distortion of the surface is expressed as:

$$r = R(t) + a_n(t)Y_n(\theta,\phi) \tag{1}$$

Where $R(t)$ is the bubble radius and Y_n is a spherical harmonic of degree n. The key to predicting the instability is to calculate the development of the distortion amplitude a_n. With the assumption that the effect of viscosity is constrained within a small boundary layer around the bubble, the differential equation governing a_n is:

$$\ddot{a}_n + B_n\dot{a}_n - A_n a_n = 0 \tag{2}$$

With

$$A_n(t) = (n-1)\frac{\ddot{R}}{R} - \frac{\beta_n\sigma}{\rho_w R^3} - \frac{2\nu\dot{R}}{R^3}\left[-\beta_n + \frac{n(n-1)(n+2)}{1+2\delta/R}\right] \tag{3}$$

$$B_n(t) = \frac{3\dot{R}}{R} + \frac{2\nu}{R^2}\left[-\beta_n + \frac{n(n+2)^2}{1+2\delta/R}\right] \tag{4}$$

Where $\beta_n=(n\text{-}1)(n\text{-}1)(n+2)$ and δ is the thickness of the boundary layer, $\delta=\min(\sqrt{\upsilon/2\pi f}, R/2n)$. For acoustic-driven bubbles (ADB), the parametric instability is dominant and the threshold for bubble destabilization is reached when the maximal eigenvalue of the Floquet transition matrix for Eq. 2 is larger than one. For the laser-induced bubbles (LIB), the Rayleigh-Taylor instability is concerned and the bubble is assumed to overwhelmed by surface distortion if $|a_n| > R$ during the bubble collapse. In this paper, we only consider the case where the unstable spherical mode n =2 and investigate the instability boundary using the above criteria for ADB and LIB, respectively.

The bubble dynamics simulation employs the Gilmore model to calculate the radial oscillation of the bubble surface and take into consideration the heat and mass transfer between the bubble interior and the surrounding liquid. The details of the model are introduced elsewhere [2]. The simulation of ADB requires the knowledge of equilibrium radius R_0 at different static pressures p_0, which are provided in reference [8]. For the LIB, the simulation is initiated at the moment when the bubble expands to the maximal radius R_{max} following recombination of the laser-induced plasma. For representing different bubble sizes as a result of variation in the laser energy, we assume different R_{max} at p_0=1 bar for LIB. When investigating the influence of static pressure, the maximum radius R^*_{max} is recalculated at the new p^*_0 according to the scaling law: $R^*_{max} = R_{max}\,(1/p^*_0)^{1/3}$. In calculating the surface instability, we assume an initial perturbation of a=1 nm and solve Eq.2 with the information of $\dot{R}$ and $\ddot{R}$ from bubble dynamics simulation.

3. Results

The simulation of ADB is based on the SBSL test by Dan et al[3], where the acoustic frequency f=17.5 kHz, acoustic amplitude p_a=1.29 bar, liquid temperature T_0=21℃, and the relative air concentration $c_{air,\infty}/c_{air,0}$=23.3%. The bubble radius $R(t)$ and distortion amplitude $a(t)$ at two static pressure p_0=1.0 bar and 0.85 bar are simulated and presented in Fig.1. It confirms that the instability for this bubble belongs to the parametric type and the distortion is accumulated during the afterbounds of the bubble. Comparing the distortion amplitude at the two different static pressures, it is revealed that the instability is augmented by the decrease of p_0. The increase of a is the result of a more violent collapse of the bubble. With the decrease of p_0, the equilibrium radius R_0 increases and the bubble expands to a larger size during the rarefaction phase of the acoustic driving. In this case, the initial distortion is amplified from cycle to cycle.

* Corresponding Author: Kewen Peng, pengkw@dgut.edu.cn

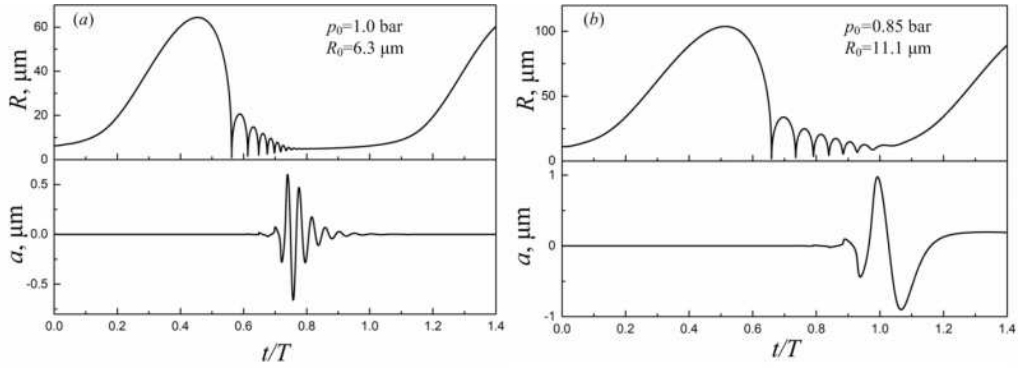

Figure 1. The development of bubble radius $R(t)$ and distortion amplitude $a(t)$ at different ambient pressures p_0 for acoustically-driven sonoluminescing bubbles: (**a**) p_0=1.0 bar; (**b**) p_0=0.85 bar. The parameters are taken from the SBSL test of Dan et al[3], i.e., f=17.5 kHz, p_a=1.29 bar, T_0=21°C, $c_{air,\infty}/c_{air,0}$=23.3%.

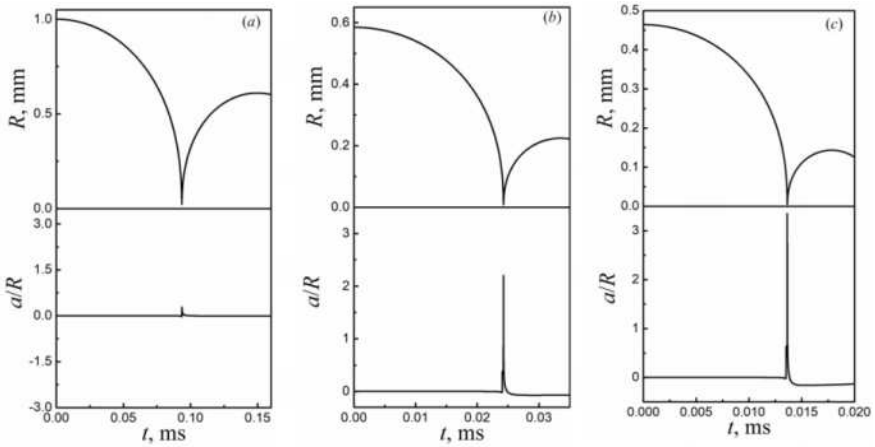

Figure 2. The development of bubble radius $R(t)$ and distortion amplitude $a(t)$ at different ambient pressures p_0 for laser-induced bubbles: (**a**) p_0=1.0 bar; (**b**) p_0=5 bar; (**c**) p_0=10 bar. The maximum radius at p_0=1.0 bar is 1 mm and decreases with the increase of p_0 as $R_{max} \propto (1/p_0^*)^{1/3}$.

For LIB, the higher static pressure would compress the bubble more strongly and increase Rayleigh-Taylor instability as shown in Fig.2, where the evolutions of bubble radius and distortion amplitude at the static pressure of 1 bar, 5 bar, and 10 bar are presented. Measured from the overwhelming criterion, it is inferred the bubble would survive from the surface distortion at p_0=1 bar but will be destroyed at p_0=5 bar and 10 bar.

By conducting large-scale parametric calculations, we scanned the acoustic parameter space and obtained the distribution of equilibrium bubble radius as displayed in Fig.2. The acoustic parameters and argon saturation in the calculation are based on the test of Dan et al[3]. The results are presented in two cases: in Case 1, the acoustic frequency is fixed at 17.5 kHz and R_0 is depicted in the p_a- p_0 space as shown in Fig.3(a); in Case 2, the ratio of p_a/p_0 is fixed at 1.41 and results are displayed in f - p_0 space in Fig.3(b). All the calculated R_0 corresponds to the relative argon saturation $c_{Ar,\infty}/c_{Ar,0}$=0.23% in water. The figure demonstrates two different variation patterns for R_0: in Case 1, the variation of R_0 is significant per the change of p_0. However, in Case 2, the equilibrium bubble radius is kept almost constant when p_0 varies in the range of 0.75-1.0 bar. The horizontal dotted line corresponds to the test conditions applied in Dan et al[3].

* Corresponding Author: Kewen Peng, pengkw@dgut.edu.cn

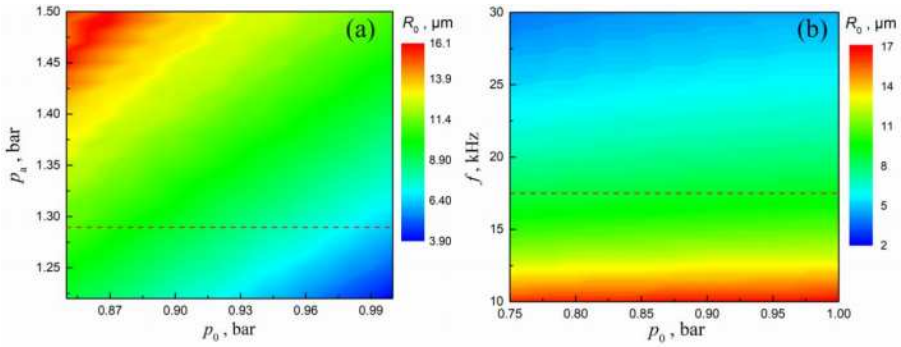

Figure 3. The distribution of R_0 in the parameter space: (**a**) The pressure amplitude-static pressure space (p_a-p_0) where the acoustic frequency f is fixed at 17.5 kHz; (**b**) The static pressure-frequency parameter space (p_0-f) where the ratio of p_a/p_0 is fixed at 1.41. Note the dotted line denotes the test parameters employed in the referenced test[3].

Based on the calculated ambient radius, we mapped the stability boundaries of the static pressure for ADB as well as for LIB as displayed in Fig.4. The range of the threshold pressure is very narrow for ADB, i.e., 0.87~1 bar, showing the sensitivity of this category of the bubble to the ambient condition. In contrast, the stability boundary for LIB is much higher and extends to as high as 5 bar. This feature demonstrates the high stability of LIB with its large size.

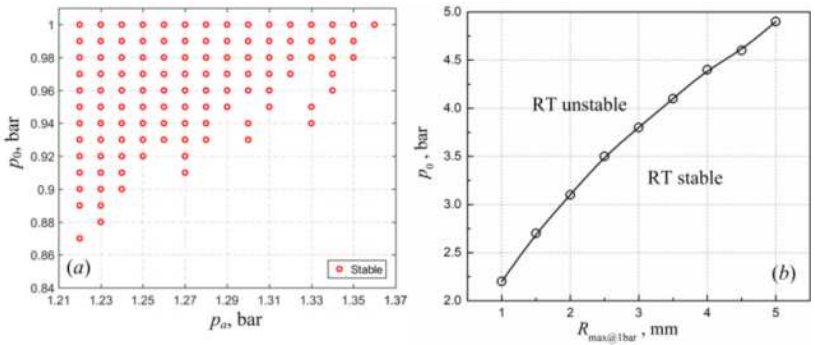

Figure 4. The stability boundaries of the static pressure for ADB (**a**) and LIB (**b**). The parameters for ADB are based on the SBSL test of Dan et al[3], see the caption of Fig.1. For the LIB, the threshold pressure is plotted against the maximum bubble radius for p_0=1 bar.

Acknowledgments: This work was supported by Foundation of State Key Laboratory of Petroleum Resources and Prospecting, China University of Petroleum, Beijing (No. PRP/open-1905), the Natural Science Foundation of Guangdong Province, China (No.2019A1515110755), National Key R&D Program of China (No.2016YFD04003032), and National Natural Science Foundation of China (Nos. 21376052 and 41961144026).

References

[1] D.F. Gaitan, L.A. Crum, C.C. Church, R.A. Roy, Sonoluminescence and bubble dynamics for a single, stable, cavitation bubble, The Journal of the Acoustical Society of America, 91 (1992) 3166-3183.
[2] K. Peng, F.G.F. Qin, R. Jiang, S. Kang, Interpreting the influence of liquid temperature on cavitation collapse intensity through bubble dynamic analysis, Ultrasonics Sonochemistry, 69 (2020) 105253.
[3] M. Dan, J. Cheeke, L. Kondic, Ambient pressure effect on single-bubble sonoluminescence, Physical Review Letters, 83 (1999) 1870.
[4] O. Baghdassarian, B. Tabbert, G.A. Williams, Luminescence characteristics of laser-induced bubbles in water, Physical review letters, 83 (1999) 2437.
[5] B. Wolfrum, T. Kurz, O. Lindau, W. Lauterborn, Luminescence of transient bubbles at elevated ambient pressures, Physical Review E, 64 (2001) 046306.
[6] S. Hilgenfeldt, D. Lohse, M.P. Brenner, Phase diagrams for sonoluminescing bubbles, Physics of fluids, 8 (1996) 2808-2826.
[7] Y. Hao, A. Prosperetti, The effect of viscosity on the spherical stability of oscillating gas bubbles, Physics of Fluids, 11 (1999) 1309-1317.
[8] K. Peng, F.G.F. Qin, S. Tian, Y. Zhang, An inverse method to fast-track the calculation of phase diagrams for sonoluminescing bubbles, submitted to *Ultrasonics Sonochemistry*.

* Corresponding Author: Kewen Peng, pengkw@dgut.edu.cn

CAV2021
11th International Symposium on Cavitation
May 10-13, 2021, Daejon, Korea

* Corresponding Author: Kewen Peng, pengkw@dgut.edu.cn